On Adaptive Fractional Dynamic Sliding Mode Control of Suspension System

Ali Karami-Mollaee [1] and Oscar Barambones [2],*

[1] Electrical and Computer Engineering Faculty, Hakim Sabzevari University, Sabzevar 9617976487, Iran; karami@hsu.ac.ir
[2] Automatic Control and System Engineering Department, University of the Basque Country, UPV/EHU, Nieves Cano 12, 01006 Vitoria-Gasteiz, Spain
* Correspondence: oscar.barambones@ehu.eus

Abstract: This paper introduces a novel adaptive control method for suspension vehicle systems in response to road disturbances. The considered model is based on an active symmetry quarter car (SQC) fractional order suspension system (FOSS). The word symmetry in SQC refers to the symmetry of the suspension system in the front tires or the rear tires of the car. The active suspension controller is generally driven by an external force like a hydraulic or pneumatic actuator. The external force of the actuator is determined using fractional dynamic sliding mode control (FDSMC) to counteract road disturbances and eliminate the chattering caused by sliding mode control (SMC). In FDSMC, a fractional integral acts as a low-pass filter before the system actuator to remove high-frequency chattering, necessitating an additional state for FDSMC implementation assuming all FOSS state variables are available but the parameters are unknown and uncertain. Hence, an adaptive procedure is proposed to estimate these parameters. To enhance closed-loop system performance, an adaptive proportional-integral (PI) procedure is also employed, resulting in the FDSMC-PI approach. A comparison is made between two SQC suspension system models, the fractional order suspension system (FOSS) and the integer order suspension system (IOSS). The IOSS controller is based on dynamic sliding mode control (DSMC) and a PI procedure (DSMC-PI). The results show that FDSMC outperforms DSMC.

Keywords: fractional order suspension system (FOSS); fractional dynamic sliding mode control (FDSMC); symmetry quarter car (SQC); proportional-integral (PI) procedure; adaptive parameter

MSC: 93C10

1. Introduction

When designing a suspension system, it is crucial to balance passenger comfort and vehicle handling [1,2]. For passenger comfort, the suspension should be soft to minimize body displacement and acceleration. Conversely, for good vehicle handling, the suspension needs to be stiff to ensure the tires maintain contact with the road in different conditions of the terrain [2,3]. In other words, for good handling of the vehicle, the tire should stick to the road [4]. In passive suspension systems, the mass–spring–damper parameters are fixed, causing the vehicle body to oscillate with the road terrain [5]. This means vibrations are transmitted from the wheels to the vehicle body [6]. However, an active symmetry quarter car (SQC) suspension system can adapt to varying road conditions, reducing both body

displacement and acceleration [7]. As we mentioned in the abstract, the word symmetry in SQC refers to the symmetry of the suspension system in the front or rear tires of the car.

Active suspension systems typically include actuators that provide additional forces, such as hydraulic [4] or pneumatic (air) [8], which are determined by feedback control [9]. Numerous studies have explored various control strategies for designing active suspension systems [10–30], including H-infinity control [9], optimal control [10], fuzzy control [11,12], neural network (NN) [13], linear quadratic regulator (LQR) or linear quadratic Gaussian (LQG) control [14–16], model-free control [17], proportional-integral-derivative (PID) control [18,19], and sliding mode control (SMC) [26–30].

Intelligent approaches such as the fuzzy controller [12] or neural networks [13] can be adaptive but commonly are not robust. In the anthers methods such as PID [19], coefficients can be self-tuned or chosen using the Ziegler–Nichols approach [20]. Algorithms like particle swarm optimization (PSO) [21] and genetic algorithms (GA) [22] have been used to tune PID parameters, improving the dynamic performance and stability of active suspension systems. In [23], fractional order PID controllers were designed using an artificial bee colony algorithm with objective functions such as integral absolute error, integral square error and integral time absolute error. Moreover, [24] analyzed a fuzzy-based PID controller for a half car active suspension system. In this analysis, the suspension's working space is the criterion under observation. In designing an LQR controller, the selection of weighting matrices is a key issue that directly affects the control action. In [25], the authors presented an approach to the optimal control problem where weighting matrices are not selected by trial and error but are calculated for the time domain.

Despite these advancements, many SMC-based suspension controllers still experience chattering, and in most of the proposed SMC suspension controller approaches, chattering occurs [26–30]. To address this, several methods were proposed [31], such as SMC-based boundary layer (BL) [32], adaptive boundary layer (ABL) [33–35], higher-order SMC (HOSMC) [36,37], and dynamic SMC (DSMC) [38,39]. While BL and ABL approaches may lose the invariance property [31,32], HOSMC requires an observer to estimate higher-order derivatives of the system model [40–43]. DSMC mitigates the discontinuous Signum function effect with a low-pass integrator filter, increasing the states that need to be estimated by an observer [38,39], making it preferable.

Given the unknown and uncertain road terrain, a robust controller is necessary [4]. This paper proposes DSMC for suspension systems to handle model uncertainty, prevent chattering and preserve invariance. The model is based on a fractional order suspension system (FOSS) for a symmetry quarter car (SQC), controlled with FDSMC combined with a PI approach (FDSMC-PI). Both FOSS and PI parameters are adaptively calculated. A comparison with the integer order suspension system (IOSS), controlled by adaptive DSMC and PI (DSMC-PI), shows that FDSMC performs better. Lyapunov's theory is used to prove the stability of the approaches.

Section 2 provides an overview of fractional derivatives and describes the IOSS and FOSS models. Section 3 presents the background and problem to clarify the proposed FDSMC and FDSMC-PI approaches. In this section, the proposed adaptive structures are also explained. Sections 4 and 5 cover the simulation results and the conclusions, respectively.

2. Preliminaries of Fractional Model Construction

In this section, we first explain a brief about the fractional derivative and then the suspension system model of SQC is presented.

2.1. Preliminaries of Fractional Calculus

Definition 1. *Caputo q-order differentiation of function f(t) with respect to time t denoted by [44,45]:*

$$D_{t_0}^q f(t) = \frac{1}{\Gamma(1-q)} \int_{t_0}^{t} \frac{f'(\tau)}{(t-\tau)^q} d\tau \tag{1}$$

where $t > t_0$, $0 < q < 1$ *and* $\Gamma(q)$ *are the Gamma function defined as* $\Gamma(q) = \int_0^\infty \tau^{q-1} e^{-\tau} d\tau$.

Lemma 1. *For any vector* $x(t) = [x_1(t), x_2(t), \ldots, x_n(t)]^T \in R^{n \times 1}$ *and any arbitrary matrix* $M \in R^{n \times n}$ *with constant elements, we have [44]:*

$$D_{t_0}^q (x^T M x) \le (D_{t_0}^q x)^T M x + x^T M (D_{t_0}^q x) \tag{2}$$

A result of this lemma can be written as follows:

$$D_{t_0}^q (x^T x) \le (D_{t_0}^q x)^T x + x^T (D_{t_0}^q x) \tag{3}$$

Remark 1. *From here and in the continuation of this paper, we suppose that the initial time of fractional derivative is zero, i.e.,* $t_0 = 0$*. Moreover, for simplicity, the subscript* t_0 *is also eliminated and hence we write* D^q *instead of* $D_{t_0}^q$.

2.2. Suspension Model Construction

The dynamic model of an SQC integer order suspension system (IOSS) is as follows [4]:

$$m_s \ddot{z}_s = -b_s(\dot{z}_s - \dot{z}_u) - k_s(z_s - z_u) + f_a \tag{4}$$

$$m_u \ddot{z}_u = +b_s(\dot{z}_s - \dot{z}_u) + k_s(z_s - z_u) - f_a + b_t(\dot{z}_r - \dot{z}_u) + k_t(z_r - z_u) \tag{5}$$

where z_s, z_u and z_r are displacement of the body, wheel and road (terrain), respectively. The first and second derivatives of z_s and z_u are velocity and acceleration. Moreover, m_s, m_u, k_s, k_t, b_s and b_t are mass, stiffness and damping rate of the body (sprung) and wheel (un-sprung), respectively. Moreover, $z_s - z_u$ is the suspension deflection and $z_u - z_r$ is the tire (wheel) deflection. Variable f_a is the output force of the hydraulic actuator which is placed between the body and the wheel. When $f_a = 0$, the suspension system acts passively or we have the passive suspension system (PSS). The aim of an active suspension system (ASS) is to determine a suitable (desired) value for f_a such that the smallest possible values for z_s, $\dot{z}_s$ and $\ddot{z}_s$ are achieved. We assumed that all the parameters are unavailable but the variables are were measurable except z_r and its derivative, which are considered as the disturbance. The dynamics of this system are represented in Figure 1.
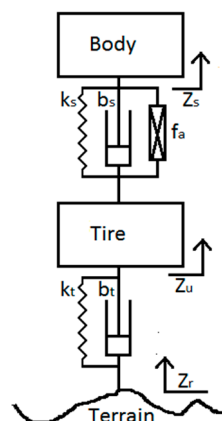
Figure 1. SQC suspension system.

Now, consider the following SQC fractional order suspension system (FOSS), which is the fractional model of Equations (4) and (5) [46].

$$m_s D^{2q} z_s = -b_s(D^q z_s - D^q z_u) - k_s(z_s - z_u) + f_a \tag{6}$$

$$m_u D^{2q} z_u = +b_s(D^q z_s - D^q z_u) + k_s(z_s - z_u) - f_a + b_t(D^q z_r - D^q z_u) + k_t(z_r - z_u) \tag{7}$$

As we mentioned, all variables are measurable except z_r. Now, we define the following available state variables:

$$x_1 = z_s, \ x_2 = D^q z_s, \ y_1 = z_u, \ y_2 = D^q z_u \tag{8}$$

then:

$$\begin{aligned} D^q x_1 &= x_2 \\ D^q x_2 &= -\frac{b_s}{m_s} x_2 - \frac{k_s}{m_s} x_1 + \frac{b_s}{m_s} y_2 + \frac{k_s}{m_s} y_1 + \frac{1}{m_s} f_a \end{aligned} \tag{9}$$

$$\begin{aligned} D^q y_1 &= y_2 \\ D^q y_2 &= +\frac{b_s}{m_u} x_2 + \frac{k_s}{m_u} x_1 - \frac{b_s}{m_u} y_2 - \frac{k_s}{m_u} y_1 - \frac{1}{m_u} f_a - \frac{b_t}{m_u} y_2 - \frac{k_t}{m_u} y_1 + f_{dist} \end{aligned} \tag{10}$$

and f_{dis} is considered an unknown disturbance.

$$f_{dist} = +\frac{b_t}{m_u} D^q z_r + \frac{k_t}{m_u} z_r \tag{11}$$

3. Proposed Adaptive FDSMC Design

Now, we define the following measurable extra variable:

$$x_3 = D^q x_2 \tag{12}$$

Moreover, we define the following sliding variable:

$$s_x = L_1 x_1 + L_2 x_2 + L_3 x_3 \tag{13}$$

where the fixed numbers L_1, L_2 and L_3 are the coefficients of sliding variable. The selection method of these parameters is explained in Remark 2.

Now, the sliding variable fractional derivative is as:

$$D^q s_x = L_1 D^q x_1 + L_2 D^q x_2 + L_3 D^q x_3 = L_1 x_2 + L_2 x_3 + L_3 D^q x_3 \tag{14}$$

then one can write:

$$D^q x_3 = -\frac{b_s}{m_s} x_3 - \frac{k_s}{m_s} x_2 + \frac{b_s}{m_s} D^q y_2 + \frac{k_s}{m_s} y_2 + \frac{1}{m_s} D^q f_a \tag{15}$$

Using Equation (10) results in:

$$\begin{aligned} D^q x_3 &= -\frac{b_s}{m_s} x_3 - \frac{k_s}{m_s} x_2 + \frac{k_s}{m_s} y_2 + \frac{1}{m_s} D^q f_a \\ &\quad + \frac{b_s}{m_s}\left(+\frac{b_s}{m_u} x_2 + \frac{k_s}{m_u} x_1 - \frac{b_s}{m_u} y_2 - \frac{k_s}{m_u} y_1 - \frac{1}{m_u} f_a - \frac{b_t}{m_u} y_2 - \frac{k_t}{m_u} y_1 + f_{dist}\right) \\ &= \left(-\frac{b_s}{m_s}\right) x_3 + \left(-\frac{k_s}{m_s} + \frac{b_s}{m_s}\frac{b_s}{m_u}\right) x_2 + \left(+\frac{b_s}{m_s}\frac{k_s}{m_u}\right) x_1 + \left(-\frac{b_s}{m_s}\frac{b_s}{m_u} - \frac{b_s}{m_s}\frac{b_t}{m_u} + \frac{k_s}{m_s}\right) y_2 \\ &\quad + \left(-\frac{b_s}{m_s}\frac{k_s}{m_u} - \frac{b_s}{m_s}\frac{k_t}{m_u}\right) y_1 + \left(-\frac{b_s}{m_s}\frac{1}{m_u}\right) f_a + \left(\frac{1}{m_s}\right) D^q f_a + \left(\frac{b_s}{m_s}\right) f_{dist} \end{aligned} \tag{16}$$

Equation (16) can be written as follows, with the corresponding coefficients:

$$D^q x_3 = k_3 x_3 + k_2 x_2 + k_1 x_1 + k_5 y_2 + k_4 y_1 + k_6 f_a + k_f D^q f_a + k_d f_{dist} \tag{17}$$

In which $k = [k_1, k_2, k_3, k_4, k_5, k_6]$ and also $k_d = -k_3$. Moreover, the vector of the state variable is $x = [x_1, x_2, x_3, y_1, y_2, f_a]^T$, then we have:

$$D^q x_3 = kx + k_f D^q f_a + k_d f_{dist} \tag{18}$$

Then, the Equations (14) and (18) results are:

$$D^q s_x = L_1 x_2 + L_2 x_3 + L_3 (kx + k_f D^q f_a + k_d f_{dist}) \tag{19}$$

Suppose that the coefficient vector k and coefficient scalars k_f and k_d are unknown and are estimated by $\hat{k}$, $\hat{k}_f$ and $\hat{k}_d$ such that $\hat{k} = [\hat{k}_1, \hat{k}_2, \hat{k}_3, \hat{k}_4, \hat{k}_5, \hat{k}_6]$. Then, the estimation of Equation (20) is as follows:

$$D^q \hat{s}_x = L_1 x_2 + L_2 x_3 + L_3 (\hat{k}x + \hat{k}_f D^q f_a + \hat{k}_d f_{dist}) \tag{20}$$

Theorem 1. *The following FDSMC control input causes the closed-loop system to be stable.*

$$D^q f_a = -\frac{L_1 x_2 + L_2 x_3 + L_3 \hat{k}x + \lambda_1 \text{sign}(s_x)}{L_3 \hat{k}_f} \tag{21}$$

If the parameters $\hat{k}$ and $\hat{k}_f$ are calculated from the following adaptive procedure:

$$\begin{aligned} D^q \hat{k} &= \gamma_1 L_3 s_x x \\ D^q \hat{k}_f &= \gamma_2 L_3 s_x D^q f_a \end{aligned} \tag{22}$$

and also:

$$\lambda_1 = L_3 k_d F_{dist} + \eta \tag{23}$$

in which $|f_{dist}| \leq F_{dist}$ and η is a positive number.

Proof. Replacing Equation (21) into Equation (20) results in:

$$D^q \hat{s}_x = -\lambda_1 \text{sign}(s_x) + L_3 \hat{k}_d f_{dist} \tag{24}$$

or:

$$L_1 x_2 + L_2 x_3 + L_3 (\hat{k}x + \hat{k}_f D^q f_a + \hat{k}_d f_{dist}) = -\lambda_1 \text{sign}(s_x) + L_3 \hat{k}_d f_{dist} \tag{25}$$

or:

$$\begin{aligned} L_1 x_2 + L_2 x_3 + L_3 (kx + k_f D^q f_a + k_d f_{dist}) - L_3 (kx + k_f D^q f_a + k_d f_{dist}) \\ + L_3 (\hat{k}x + \hat{k}_f D^q f_a) = -\lambda_1 \text{sign}(s_x) \end{aligned} \tag{26}$$

From Equations (19) and (26), the next equation is obtained:

$$D^q s_x = L_3 (k - \hat{k})x + L_3 (k_f - \hat{k}_f) D^q f_a + L_3 k_d f_{dist} - \lambda_1 \text{sign}(s_x) \tag{27}$$

Defining $\widetilde{k} = k - \hat{k}$ and $\widetilde{k}_f = k_f - \hat{k}_f$ results in:

$$D^q s_x = -\lambda_1 \text{sign}(s_x) + L_3 \widetilde{k}x + L_3 \widetilde{k}_f D^q f_a + L_3 k_d f_{dist} \tag{28}$$

Now, consider the following Lyapunov function:

$$V(t) = \frac{1}{2} s_x{}^2 + \frac{1}{2\gamma_1} \widetilde{k}\widetilde{k}^T + \frac{1}{2\gamma_2} \widetilde{k}_f^2 \tag{29}$$

Based on Lemma 1, one can conclude that:

$$D^q V(t) \leq s_x D^q s_x - \frac{1}{\gamma_1} \widetilde{k} D^q \hat{k} - \frac{1}{\gamma_2} \widetilde{k}_f D^q \hat{k}_f \tag{30}$$

Therefore:

$$
\begin{aligned}
D^q V(t) &\leq s_x \left(-\lambda_1 \text{sign}(s_x) + L_3 \widetilde{k} x + L_3 \widetilde{k}_f D^q f_a + L_3 k_d f_{dist} \right) \\
&\quad - \frac{1}{\gamma_1} \widetilde{k}(\gamma_1 L_3 s_x x) - \frac{1}{\gamma_2} \widetilde{k}_f (\gamma_2 L_3 s_x D^q f_a) \\
&= -\lambda_1 s_x \text{sign}(s_x) + L_3 k_d f_{dist} s_x \leq -\lambda_1 |s_x| + L_3 k_d |f_{dist}| \, |s_x| \\
&\leq (-\lambda_1 + L_3 k_d F_{dist}) \, |s_x|
\end{aligned}
\tag{31}
$$

Using Equation (23) results in:

$$D^q V(t) \leq -\eta |s_x| \tag{32}$$

When using the Lyapunov stability theory, it is concluded that the closed-loop system is stable and proof of the theorem is completed. $\square$

Theorem 2. *The following FDSMC-PI control input causes the closed-loop system to be stable.*

$$
\begin{aligned}
D^q f_a &= -\frac{L_1 x_2 + L_2 x_3 + L_3 \hat{k} x + \lambda_1 \text{sign}(s_x) + u_{PI}}{L_3 \hat{k}_f} \\
u_{PI} &= \hat{k}_P s_x + \hat{k}_I \int_0^t s_x dt
\end{aligned}
\tag{33}
$$

If the adaptive parameters are calculated from the following procedure:

$$
\begin{aligned}
D^q \hat{k} &= \gamma_1 L_3 s_x x \\
D^q \hat{k}_f &= \gamma_2 L_3 s_x D^q f_a \\
D^q \hat{k}_P &= \eta_1 s_x^2 \\
D^q \hat{k}_I &= \eta_2 s_x \int_0^t s_x dt
\end{aligned}
\tag{34}
$$

Also, as in the previous theorem:

$$\lambda_1 = L_3 k_d F_{dist} + \eta \tag{35}$$

in which $|f_{dist}| \leq F_{dist}$ *and* η *is a positive number.*

Proof. Replacing Equation (33) into Equation (20) and as with Equation (24) to Equation (28), one can conclude that:

$$D^q s_x = -\lambda_1 \text{sign}(s_x) + L_3 \widetilde{k} x + L_3 \widetilde{k}_f D^q f_a + L_3 k_d f_{dist} - u_{PI} \tag{36}$$

Now, consider the following Lyapunov function:

$$V(t) = \frac{1}{2} s_x^2 + \frac{1}{2\gamma_1} \widetilde{k} \widetilde{k}^T + \frac{1}{2\gamma_2} \widetilde{k}_f^2 + \frac{1}{2\eta_1} \hat{k}_P^2 \frac{1}{2\eta_2} \hat{k}_I^2 \tag{37}$$

Based on Lemma 1, one can conclude that:

$$D^q V(t) \leq s_x D^q s_x - \frac{1}{\gamma_1} \widetilde{k} D^q \hat{k} - \frac{1}{\gamma_2} \widetilde{k}_f D^q \hat{k}_f + \frac{1}{\eta_1} \hat{k}_P D^q \hat{k}_P + \frac{1}{\eta_2} \hat{k}_I D^q \hat{k}_I \tag{38}$$

Therefore:

$$
\begin{aligned}
D^q V(t) &\leq s_x \left(-\lambda_1 \text{sign}(s_x) + L_3 \widetilde{k} x + L_3 \widetilde{k}_f D^q f_a + \hat{k}_P s_x - \hat{k}_I \int_0^t s_x dt - L_3 k_d f_{dist} \right) \\
&\quad - \frac{1}{\gamma_1} \widetilde{k}(\gamma_1 L_3 s_x x) - \frac{1}{\gamma_2} \widetilde{k}_f (\gamma_2 L_3 s_x D^q f_a) + \frac{1}{\eta_1} \hat{k}_P (\eta_1 s_x^2) + \frac{1}{\eta_2} \hat{k}_I \left(\eta_2 s_x \int_0^t s_x dt \right) \\
&= -\lambda_1 s_x \text{sign}(s_x) + L_3 k_d f_{dist} s_x \leq -\lambda_1 |s_x| + L_3 k_d |f_{dist}| \, |s_x| \leq (-\lambda_1 + L_3 k_d F_{dist}) \, |s_x|
\end{aligned}
\tag{39}
$$

Using the Equation (35) results:

$$D^q V(t) \leq -\eta |s_x| \tag{40}$$

When using the Lyapunov stability theory, it is concluded that the closed-loop system is stable and proof of the theorem is completed. □

4. Simulation Presentation

In this section, two simulations are carried out, DSMC and FDSMC. The parameters of the suspension system have been chosen as in Table 1 [4].

Table 1. The parameters of suspension system.

Parameter	Value	Unit
m_s	243	kg
m_u	40	kg
b_s	370	N/(m/s)
b_t	414	N/(m/s)
k_s	14,671	N/m
k_t	124,660	N/m

In addition, the parameters of the controllers have been selected as:

$$L_1 = 4, \; L_2 = 0.4, \; L_3 = 0.01, \; \lambda_1 = 2 \tag{41}$$

Remark 2. *The sliding surface coefficients L_1, L_2 and L_3 are selected such that the internal dynamics of the sliding surface (13) are considered to be zero, i.e., in the case of $s_x = 0$, all the state variables x_1, x_2 and x_3 converge to zero. Also, we selected $\gamma_1 = \gamma_2 = \eta_1 = \eta_2 = 1$ in Equation (34) to have a moderate convergence and to reduce drift of adaptive parameters and moreover, for a good approximate of function kx in Equation (18).*

Moreover, based on the previous discussion, the structure of the proposed controller is shown and depicted in Figure 2.
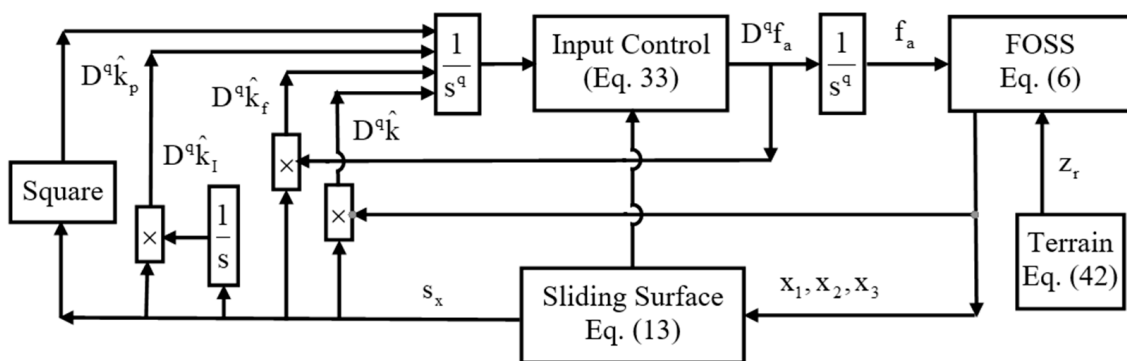
Figure 2. Block diagram of the proposed FDSMC-PI.

As this figure shows, before the input control of the suspension system (FOSS), a fractional integrator is placed to suppress the chattering produced by the SMC in Equation (33). Moreover, the unknown parameters of the system are calculated using the adaptive parameters of Equation (34). To provide these adaptive parameters, a new fractional integrator is needed.

However, the advantages of this approach (like the chattering elimination) are promising for practical applications because it is clear that the low-pass integrator removes all the high frequency produced due to chattering.

The road terrain in Figure 3 is obtained using the following equation, which consists of two triangular-like functions. Considerations such as this terrain are common in the literature [4,6].

$$z_r = \begin{cases} 0.1\sin(t) & : 6 \leq t \leq 7 \\ 0 & : \text{Otherwise} \end{cases} \tag{42}$$
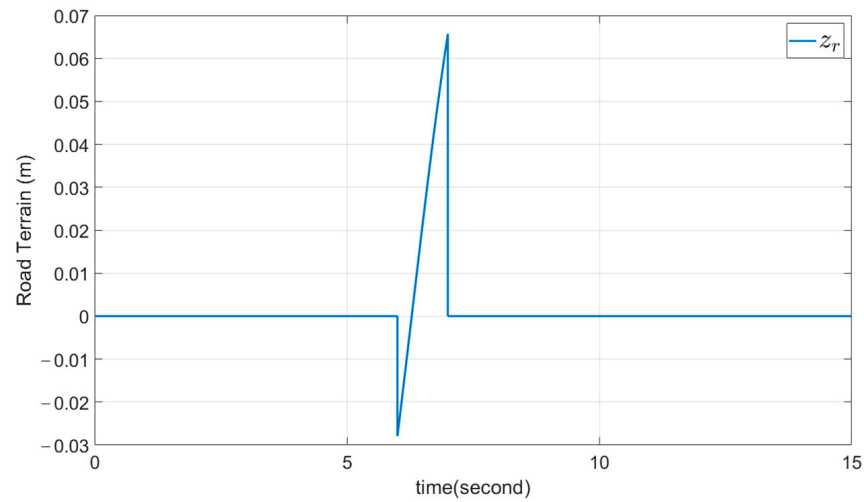
Figure 3. Disturbance road terrain.

The simulation was conducted using MATLAB with a fixed step time of 0.0001 for both the fractional dynamic sliding mode control (FDSMC-PI) and the dynamic sliding mode control (DSMC-PI). In FDSMC-PI, the fractional order is chosen as $q = 0.8$, while in DSMC-PI, it is $q = 1$ in all equations. The simulation results are depicted in Figures 4–12. Note that in all figures, the horizontal axis scaling depends on the car's velocity V according to the equation $d = Vt$, where d is displacement.
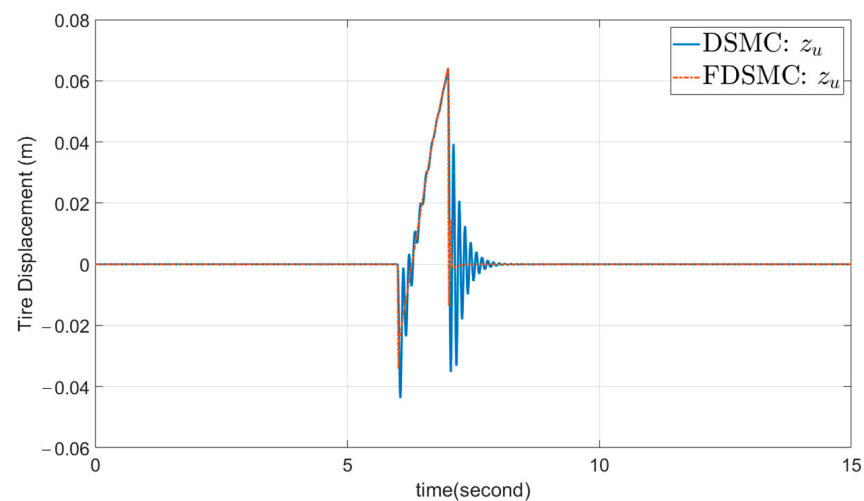
Figure 4. Vertical tire displacement.
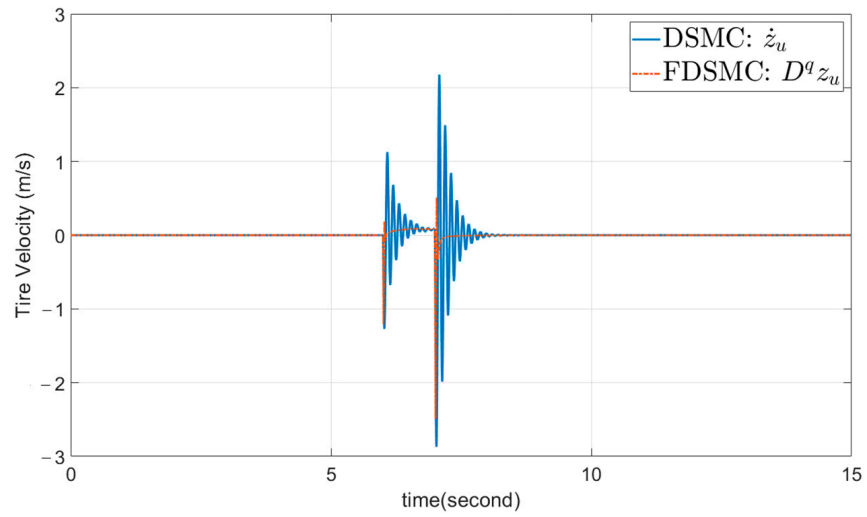
Figure 5. Vertical tire velocity.
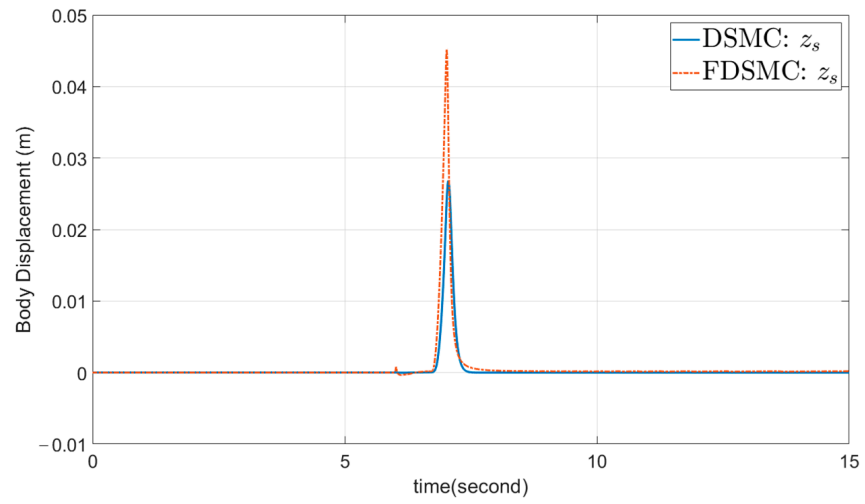
Figure 6. Vertical body displacement.
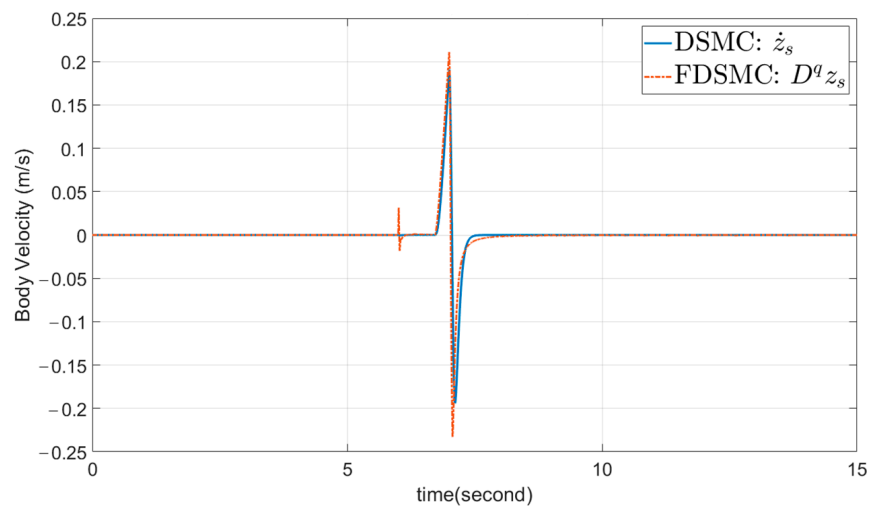
Figure 7. Vertical body velocity.
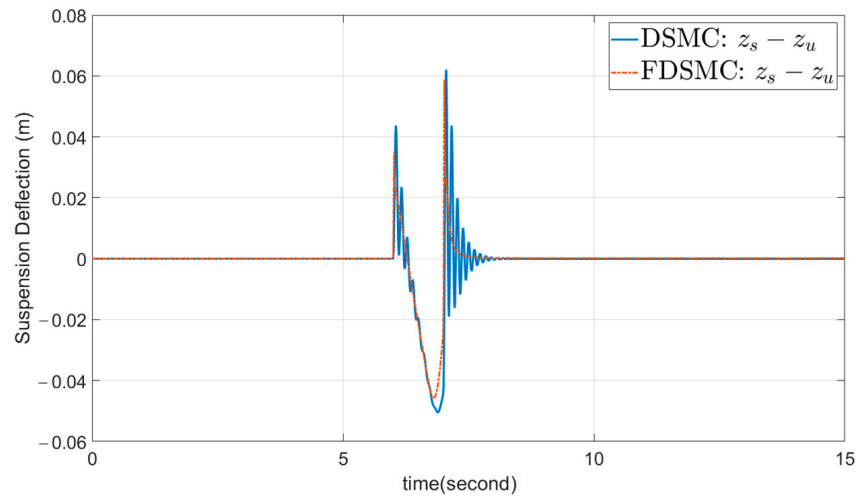
Figure 8. Vertical suspension deflection.
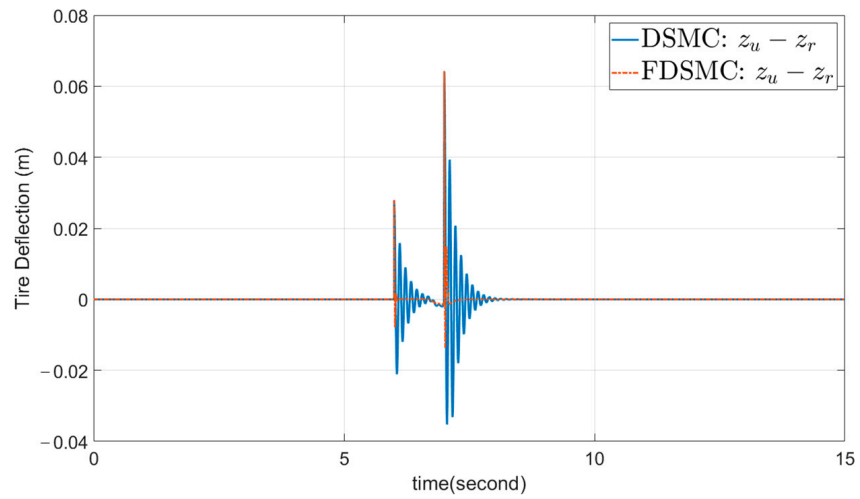
Figure 9. Vertical tire deflection.
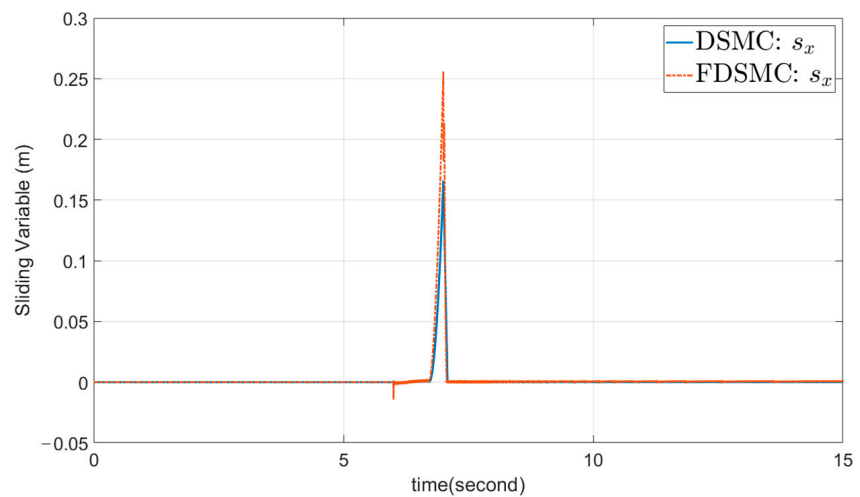
Figure 10. Sliding variable convergence.
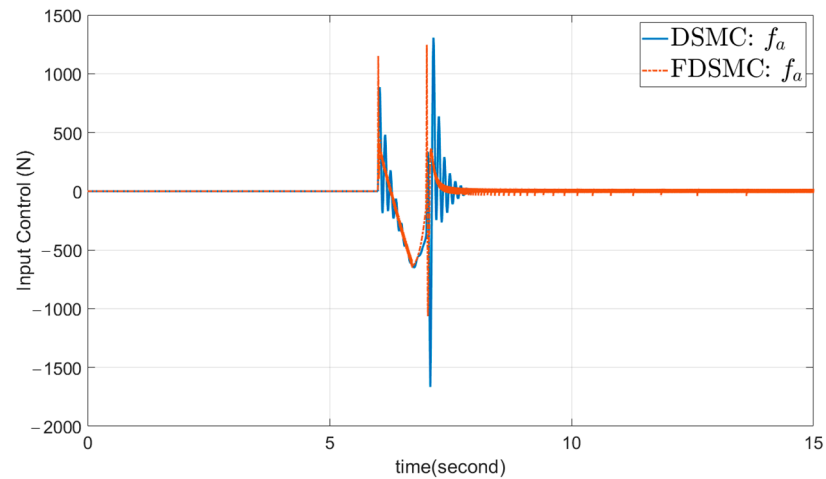
Figure 11. Force input control signal.
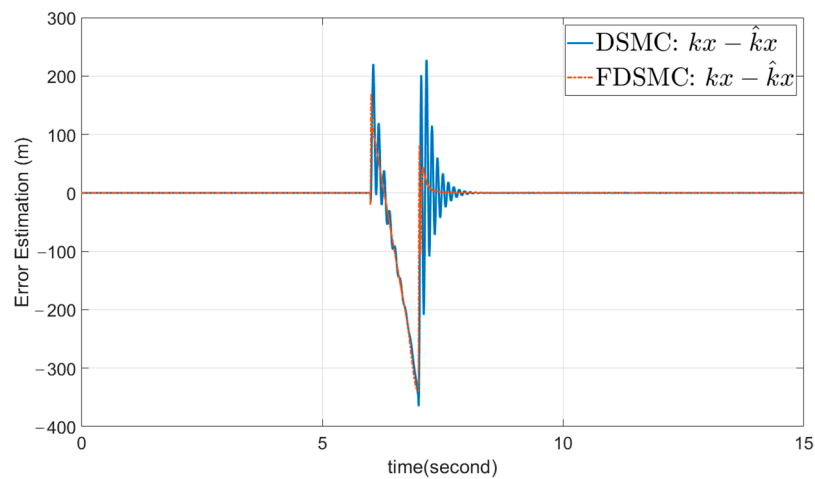
Figure 12. Function error estimation.

Figures 4 and 5 show that tire displacement and velocity exhibit vibrations in DSMC-PI but are smoother in FDSMC-PI. Additionally, body displacement and velocity are very similar in both cases, as seen in Figures 6 and 7. Figure 8 illustrates the softer suspension between the body and the tire in FDSMC-PI. Passenger comfort, shown in Figure 6, is similar in both controllers, but vehicle handling is better in FDSMC-PI, as indicated in Figures 4 and 9.

Comparing road terrain in Figure 3 with tire displacement in Figure 4, it is evident that the tire adheres to the road in FDSMC-PI, unlike in DSMC-PI. Figure 9 highlights the stiff suspension between the tire and the road in FDSMC-PI. Figure 11 displays the input force for both cases, which can be supplied by a pneumatic or hydraulic system. The sliding surface and function error estimation are shown in Figures 10 and 12, respectively. The absence of chattering in both DSMC-PI and FDSMC-PI is evident from all these figures.

The statistical comparisons of the suspension system for FDSMC-PI and DSMC-PI are provided in Table 2. These comparisons are based on the minimum (Min), maximum (Max) and root mean square (RMS) of the variables depicted in Figures 3–12. As is clear from this table, all of the statistical variables in FDSMC-PI are better than those in DSMC-PI except for z_s, $\dot{z}_s$ and s_x. This means that, generally, fractional controllers are better than integer controllers.

Table 2. The statistical comparison of suspension system.

Methods	FDSMC-PI			DSMC-PI		
Parameter	Min	Max	RMS	Min	Max	RMS
z_r	-0.0279	0.0675	0.0089	-0.0279	0.0657	0.0089
z_u	-0.0343	0.0643	0.0088	-0.0437	0.0641	0.0096
$\dot{z}_u$	-2.4921	0.5105	0.0780	-2.8705	2.1772	0.2208
z_s	-3.3888×10^{-4}	0.0452	0.0038	-1.9490×10^{-5}	0.0268	0.026
$\dot{z}_s$	-0.2328	0.2109	0.0227	-0.1940	0.1908	0.0215
$z_s - z_u$	-0.0459	0.0588	0.0078	-0.0505	0.0620	0.0092
$z_u - z_r$	-0.0137	0.0643	0.0014	-0.0352	0.0641	0.0040
s_s	-0.0143	0.2559	0.0190	-3.2425×10^{-4}	0.1661	0.0126
f_a	-1.0661×10^3	1.2461×10^3	115.5866	-1.6658×10^3	1.3065×10^3	152.4935
$kx - \hat{k}x$	-340.9504	169.3054	45.1721	-365.1951	227.6984	49.4476

5. Conclusions

The symmetry quarter car (SQC) model under consideration utilizes a fractional order suspension system (FOSS) controlled by an external force. To ensure a smooth forced signal and manage road terrain disturbances, fractional dynamic sliding mode control (FDSMC) is employed. In FDSMC, a fractional integral acts as a low-pass filter before the actuator to reduce chattering produced by sliding mode control (SMC). To enhance performance, an adaptive proportional-integral (PI) method is incorporated, resulting in the adaptive FDSMC-PI approach. For comparison, an integer order suspension system (IOSS) with dynamic sliding mode control (DSMC) and a PI method is also implemented (DSMC-PI). Assuming all parameters in both FOSS and IOSS are unknown, an adaptive procedure is used to identify the system parameters. It is demonstrated that chattering is removed in both the DSMC and the FDSMC methods. Additionally, while both approaches offer similar passenger comfort, FDSMC provides better vehicle handling due to improved tire–road adhesion.

Author Contributions: A.K.-M.: analysis, writing—original draft and preparation; O.B.: conceptualization, writing—review and editing. All authors have read and agreed to the published version of the manuscript.

Data Availability Statement: The original contributions presented in the study are included in the article, further inquiries can be directed to the corresponding author.

Conflicts of Interest: The authors declare no conflicts of interest.

References

1. Yim, Y.U.; Oh, S.Y. Modeling of vehicle dynamics from real vehicle measurements using a neural network with two-stage hybrid learning for accurate long-term prediction. *IEEE Trans. Veh. Technol.* **2004**, *53*, 1076–1084. [CrossRef]
2. Chen, B.-C.; Shiu, Y.-H.; Hsieh, A.-C. Sliding-mode control for semi-active suspension with actuator dynamics. *Veh. Syst. Dyn.* **2011**, *4*, 277–290. [CrossRef]
3. Yoshimura, T.; Kume, A.; Kurimoto, M.; Hino, J. Construction of an active suspension system of a quarter car model using the concept of sliding mode control. *J. Sound Vib.* **2001**, *239*, 187–199. [CrossRef]

4.   Karami-Mollaee, A. Design of dynamic sliding mode controller for active suspension system. *Modares Mech. Eng.* **2016**, *16*, 51–58.

5.   Huang, S.-J.; Chen, H.-Y. Adaptive sliding controller with self-tuning fuzzy compensation for vehicle suspension control. *Mechatronics* **2006**, *16*, 607–622. [CrossRef]

6.   Nguyen, D.N.; Nguyen, T.A. Proposing an original control algorithm for the active suspension system to improve vehicle vibration: Adaptive fuzzy sliding mode proportional-integral-derivative tuned by the fuzzy (AFSPIDF). *Heliyon* **2023**, *9*, 4210. [CrossRef]

7.   Du, H.; Zhang, N. H∞ control of active vehicle suspensions with actuator time delay. *J. Sound Vib.* **2007**, *301*, 236–252. [CrossRef]

8.   Zhang, J.; Yang, Y.; Hu, C. An adaptive controller design for nonlinear active air suspension systems with uncertainties. *Mathematics* **2023**, *11*, 2626–2638. [CrossRef]

9.   Chantranuwathana, S.; Peng, H. Adaptive robust force control for vehicle active suspensions. *Int. J. Adapt. Control. Signal Process.* **2004**, *18*, 83–102. [CrossRef]

10.   Corona, D.; Giua, A.; Seatzu, C. Optimal control of hybrid automata: An application to the design of a semi active suspension. *Cont. Eng. Pract.* **2004**, *12*, 1305–1318. [CrossRef]

11.   Sharkawy, A.B. Fuzzy and adaptive fuzzy control for the automobiles' active suspension system. *Veh. Syst. Dyn.* **2005**, *43*, 795–806. [CrossRef]

12.   Fu, S.; Liu, M.; Wu, H.; Liang, X.; Zeng, X. Active disturbance rejection control based on BP neural network for suspension system of electromagnetic suspension vehicle. *Int. J. Dyn. Contr.* **2025**, *13*, 1–13. [CrossRef]

13.   Mahmoodabadi, M.J.; Nejadkourki, N.; Ibrahim, M.Y. Optimal fuzzy robust state feedback control for a five DOF active suspension system. *Results Contr. Opt.* **2024**, *17*, 100504. [CrossRef]

14.   Sohn, H.C.; Hong, K.T.; Hong, K.S.; Yoo, W.S. An adaptive LQG control for semi-active suspension systems. *Int. J. Veh. Des.* **2004**, *34*, 309–326. [CrossRef]

15.   Nguyen, M.L.; Tran, T.T.H.; Nguyen, T.A.; Nguyen, D.N.; Dang, N.D. Application of MIMO control algorithm for active suspension system: A new model with 5 state variables. *Lat. Am. J. Solid. Struct.* **2022**, *19*, e435. [CrossRef]

16.   Xia, R.X.; Li, J.H.; He, J.; Shi, D.F.; Zhang, Y. Linear-Quadratic-Gaussian controller for truck active suspension based on cargo integrity. *Adv. Mech. Eng.* **2015**, *7*, 1687814015620320. [CrossRef]

17.   Swevers, J.; Lauwerys, C.; Vandersmissen, B.; Maes, M.; Reybrouck, K.; Sas, P. A model free control structure for the on-line tuning of the semi-active suspension of a passenger car. *Mech. Sys. Signal Proc.* **2007**, *21*, 1422–1436. [CrossRef]

18.   Nguyen, T.A. Improving the comfort of the vehicle based on using the active suspension system controlled by the double-integrated controller. *Shock Vib.* **2021**, *2021*, 1426003. [CrossRef]

19.   Mahmoodabadi, M.J.; Nejadkourki, N. Optimal fuzzy adaptive robust PID control for an active suspension system. *Aust. J. Mech. Eng.* **2022**, *20*, 681–691. [CrossRef]

20.   Nguyen, T.A. Control the hydraulic stabilizer bar to improve the stability of the vehicle when steering. *Math. Model. Eng. Prob.* **2021**, *8*, 199–206. [CrossRef]

21.   Metered, H.; Elsawaf, A.; Vampola, T.; Sika, Z. Vibration control of MR-damped vehicle suspension system using PID controller tuned by particle swarm optimization. *SAE Int. J. Passeng. Cars–Mech. Sys.* **2015**, *8*, 426–435. [CrossRef]

22.   Niu, X.J. The optimization for PID controller parameters based on genetic algorithm. *Appl. Mech. Mater.* **2014**, *513*, 4102–4105. [CrossRef]

23.   Kesarkar, A.A.; Selvaganesan, N. Tuning of optimal fractional-order PID controller using an artificial bee colony algorithm. *Sys. Sci. Contr. Eng.* **2015**, *3*, 99–105. [CrossRef]

24.   Khodadadi, H.; Ghadiri, H. Self-tuning PID controller design using fuzzy logic for half car active suspension system. *Int. J. Dyn. Contr.* **2018**, *6*, 224–232. [CrossRef]

25.   Oral, Ö.; Çetin, L.; Uyar, E. A novel method on selection of Q and R matrices in the theory of optimal control. *Int. J. Syst. Contr.* **2010**, *1*, 84–92.

26.   Chen, P.C.; Huang, A.C. Adaptive sliding control of non-autonomous active suspension systems with time-varying loadings. *J. Sound Vib.* **2005**, *282*, 1119–1135. [CrossRef]

27.   Chen, P.-C.; Huang, A.-C. Adaptive sliding control of active suspension systems with uncertain hydraulic actuator dynamics. *Int. J. Veh. Sys. Dyn.* **2006**, *44*, 357–368. [CrossRef]

28.   Ji, X.; Wei, W.; Su, H. A class of proportional-integral sliding mode control with application to active suspension system. *Sys. Contr. Lett.* **2007**, *56*, 253–254. [CrossRef]

29.   Ovalle, L.; Ríos, H.; Ahmed, H. Robust Control for an Active Suspension System via Continuous Sliding-Mode Controllers. *Int. J. Eng. Sci. Technol.* **2022**, *28*, 101026. [CrossRef]

30.   Nguyen, T.A. Research on the Sliding Mode–PID control algorithm tuned by fuzzy method for vehicle active suspension. *Forces Mech.* **2023**, *11*, 100206. [CrossRef]

31.   Lee, H.; Utkin, V.-I. Chattering suppression methods in sliding mode control systems. *Annu. Rev. Contr.* **2007**, *31*, 179–188. [CrossRef]

32. Fuh, C.-C. Variable-thickness boundary layers for sliding mode control. *J. Mar. Sci. Technol.* **2008**, *16*, 288–294. [CrossRef]

33. Chen, H.-M.; Renn, J.-C.; Su, J.-P. Sliding mode control with varying boundary layers for an electro-hydraulic position servo system. *Int. J. Adv. Manuf. Technol.* **2005**, *26*, 117–123. [CrossRef]

34. Zhang, X. Sliding mode-like fuzzy logic control with adaptive boundary layer for multiple-variable discrete. *J. Intell. Sys.* **2016**, *25*, 209–220. [CrossRef]

35. Allamehzadeh, H.; Cheung, J.Y. Optimal fuzzy sliding mode control with adaptive boundary layer. *WSEAS Trans. Sys.* **2004**, *3*, 1887–1892.

36. Cucuzzella, M.; Incremona, G.P.; Ferrara, A. Design of robust higher order sliding mode control for micro grids. *IEEE J. Emerg. Sel. Top. Cir. Sys.* **2015**, *5*, 393–401.

37. Karami-Mollaee, A.; Barambones, O. Higher order sliding mode control of MIMO induction motors: A new adaptive approach. *Mathematics* **2023**, *11*, 4558. [CrossRef]

38. Chen, M.-S.; Chen, C.-H.; Yang, F.-Y. An LTR-observer based dynamic sliding mode control for chattering reduction. *Automatica* **2007**, *43*, 1111–1116. [CrossRef]

39. Karami-Mollaee, A.; Tirandaz, H. Adaptive fuzzy fault tolerant control using dynamic sliding mode. *Int. J. Contr. Autom. Sys.* **2018**, *16*, 360–367. [CrossRef]

40. Levant, A. Homogeneity approach to high-order sliding mode design. *Automatica* **2005**, *41*, 823–830. [CrossRef]

41. Plestan, F.; Glumineau, A.; Laghrouche, S. A new algorithm for high-order sliding mode control. *Int. J. Robust Nonlinear Contr.* **2008**, *18*, 441–453. [CrossRef]

42. Shtessel, Y.B.; Fridman, L.; Zinober, A. Higher order sliding modes. *Int. J. Robust Nonlinear Contr.* **2008**, *18*, 381–384. [CrossRef]

43. Yang, Y.; Qin, S.; Jiang, P. A modified super-twisting sliding mode control with inner feedback and adaptive gain schedule. *Int. J. Adapt. Contr. Signal Process.* **2017**, *31*, 398–416. [CrossRef]

44. Karami-Mollaee, A.; Barambones, O. Sliding observer in sliding mode control of multi-inputs fractional order chaotic systems. *Pramana–J. Phys.* **2022**, *96*, 180–197. [CrossRef]

45. Azizi, A.; Naderi Soorki, M.; Vedadi Moghaddam, T.; Soleimanizadeh, A. A new fractional-order adaptive sliding-mode approach for fast finite-time control of human knee joint orthosis with unknown dynamic. *Mathematics* **2023**, *11*, 4511–4527. [CrossRef]

46. Chen, E.; Xing, W.; Wang, M.; Ma, W.; Chang, Y. Study on chaos of nonlinear suspension system with fractional-order derivative under random excitation. *Chaos Solitons Frac.* **2021**, *152*, 111300. [CrossRef]